UNIVERSITY OF LEEDS

This is a repository copy of *Providing adhesion for a miniture mobile intra-abdominal device based on biomimetic principles*.

White Rose Research Online URL for this paper:
http://eprints.whiterose.ac.uk/8485/

**Proceedings Paper:**
Taylor, G., Liskiewicz, T., Neville, A. et al. (3 more authors) (2009) Providing adhesion for a miniture mobile intra-abdominal device based on biomimetic principles. In: Proceedings of 3rd Vienna International Conference on Nano-Technology. Viennano'09, 18-20 March, Vienna, Austria. , pp. 401-407. ISBN 978-3-901657-32-0

**Reuse**
See Attached

**Takedown**
If you consider content in White Rose Research Online to be in breach of UK law, please notify us by emailing eprints@whiterose.ac.uk including the URL of the record and the reason for the withdrawal request.

White Rose university consortium
Universities of Leeds, Sheffield & York

eprints@whiterose.ac.uk
https://eprints.whiterose.ac.uk/

# PROVIDING ADHESION FOR A MINIATURE MOBILE INTRA-ABDOMINAL DEVICE BASED ON BIOMIMETIC PRINCIPLES

G. Taylor, T. Liskiewicz, A. Neville, A. Morina, P. H. Gaskell
Institute of Engineering Thermofluids, Surfaces & Interfaces
School of Mechanical Engineering, University of Leeds
Woodhouse Lane, Leeds, LS2 9JT, United Kingdom

D. Jayne
Academic Surgical Unit, St. James's University Hospital; Leeds, LS9 7TF, United Kingdom

## 1 Abstract

This paper investigates the surface adhesion characteristics required for a miniature mobile device to move around the abdominal cavity. Such a device must be capable of adhering to the tissue lining and move freely across the upper surface of the insufflated abdomen. Accordingly, the potential of utilising bio-inspired solutions to facilitate wet adhesion is assessed.

## 2 Introduction

Surgical practice has undergone major changes over the past two decades with the introduction of minimally invasive, or "keyhole" surgical techniques. Advantages such as post-operative pain reduction, fewer scars, quicker recovery times, reduced hospital stays and improved cost-effectiveness have resulted in relation to several types of abdominal operation [1-2]. In addition, minimally invasive techniques applicable to more complex procedures have been described and shown to be safe and effective; their true advantages, however, have yet to be realised. This is due in the main to the inherent difficulty of performing complex procedures with the instrumentation available, which is hampered by very limited dexterity, ergonomics and visual feedback [3]. These constraints have led to the recent introduction of robotic systems across a number of different surgical specialties [4]. However, while improvements in general have been achieved, the systems available currently for minimal access abdominal surgery are bulky, cumbersome and very expensive. As a result there has been a shift towards miniaturisation of surgical technology [5-6], with the ultimate aim of utilising completely internalised or 'intracorporeal' devices [7-8].

Such trends in medical and surgical research have led to collaborations between mechanical engineers and surgeons, and the investigation of interfaces between synthetic engineered materials and human tissue [9-10]. The particular tissue of interest here, with reference to the development of technology in abdominal surgery, is the peritoneum – a thin layer of cells that forms the internal surface lining of the abdominal wall. It covers also the surfaces of the abdominal organs (visceral peritoneum), and the diaphragm (parietal peritoneum). The visceral and parietal peritoneal surfaces are continuous, thereby forming a potential enclosed space known as the peritoneal cavity. During laparoscopic surgery, the peritoneal cavity is 'insufflated' with carbon dioxide to a pressure of around 15mmHg. This creates a true space within the abdomen allowing the organs to be viewed and accessed via the anterior abdominal wall. The ability of a miniature surgical device to adhere to and move across the internal surface of the abdominal wall, without causing damage, would repressent a considerable step forward in the advancement of technology for applications in minimally invasive surgery.

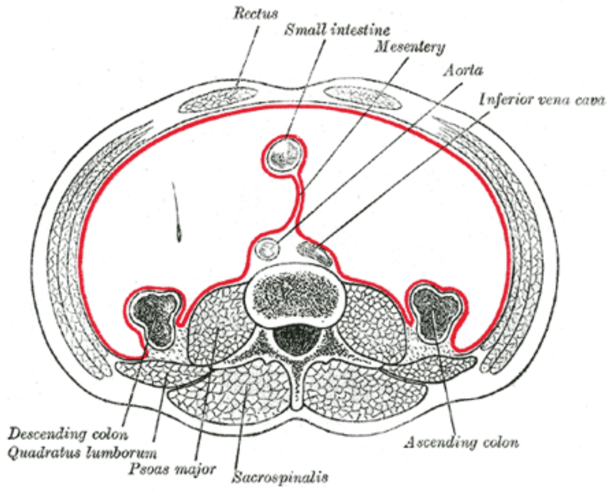


*Figure 1: Diagram of a transverse section through the abdomen – the peritoneum is represented by the dark line, and the white area is the operating space created by insufflation with carbon dioxide [11].*

The only such device currently under development, which is both mobile and independently adherent (i.e. not requiring containment within a lumen) to an internal body surface, is the HeartLander [7]. This uses suction cups and an external vacuum pump to make inch-worm movements across the surface of the heart at speeds of around $0.5mms^{-1}$. As the area of the peritoneal surface is much greater, devices required to traverse it will need to do so quickly with the proviso that minimising damage to the associated tissue will drive the need for a complementary minimally destructive adhesion mechanism.

This paper concerns a preliminary investigation as to the possibility of adhesion by capillary forces by contacting the wet peritoneal surface with a range of synthetic surfaces. Such a capability would have a wide range of potential uses within the field of minimally invasive surgery. The study forms part of a research programme aimed at developing an intra-abdominal device with the ability to traverse across the internal surface of the abdominal wall (Fig. 2).

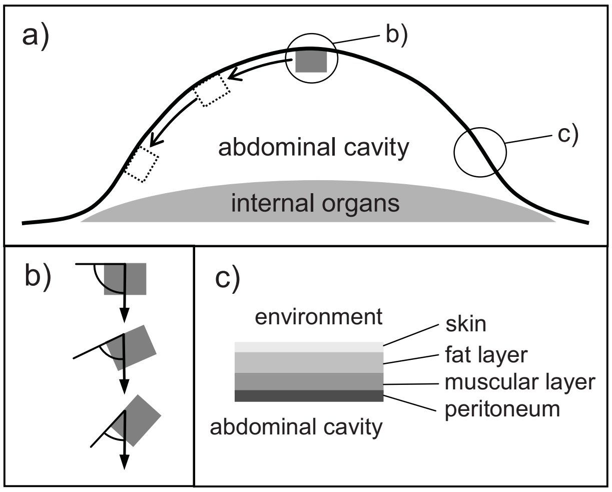


*Figure 2: Operational environment; a) insufflated abdomen showing peritoneal cavity and intra-abdominal device moving across the cavity; b) different adhesion conditions depending on the device position; c) layered structure of the cavity wall.*

To achieve adhesion and locomotion over the peritoneum a suitable contacting surface is required, which has the ability to reliably and repeatedly adhere to and detach from the peritoneum, without causing tissue damage; it must also be able to resist the shear forces when attached to a vertical or angled part of the abdominal wall. Several biomimetic solutions, based on water beetle feet [12], tree frog [13] and gecko toes [14], were considered when choosing suitable materials to investigate, the underlying principle being the exploitation of capillarity and van der Waals forces.

The exploitation of van der Waals and/or capillary forces is achieved by a range of creatures by slightly differing mechanisms [12-14]. However, all such mechanisms have in common the ability to conform with high accuracy to the opposing surface. It is this conformability which allows the small individual surface forces to be multiplied sufficiently to support the mass of the creature in question [15].

The relatively recent advances in the understanding of these mechanisms has encouraged much scientific interest in mimicking them for engineering and technological applications. Perhaps most interest has been in the development of nano and micro-pillar arrays based on the morphology of the gecko foot [16] as well as several insect species [13,17]. Obstacles to the progress of such materials have been the tendency of the fabricated pillars to bunch together and the high cost of replicating the patterns to a useable scale. However these problems are gradually being addressed.

There is also specific interest in exploiting adhesive and frictional properties of such materials for medical applications. Sitti et al. [18] are developing a micropillar array which has been shown to enhance friction on the internal intestinal surface. This will enable the manufacture of an endoscopic video capsule with the ability to stop and anchor itself within the lumen of the bowel. Also, Mahdavi et al. [19] are designing nanoscale pillar arrays to enhance the properties of an internal tissue adhesive tape to be used in the treatment of surgical and traumatic wounds.

On the underside of the abdominal wall the peritoneum provides a surface that is smooth, relatively flat and firm due to the underlying muscular layer. During abdominal surgery the patient is in a prone position. The key challenge is therefore to develop a mechanism to resist the force of gravity and allow a device to adhere to the peritoneum.

However, the abdominal wall becomes dome shaped as it is insufflated with gas prior to surgery. So in addition to the perpendicular gravitational force, the device must also resist the contribution of tangential sliding forces which increase with deviation away from the midline, as the wall curves closer towards 90 degrees (Fig. 2b).

This paper describes the methods used to evaluate the effect on these interfacial forces for the case when various man-made micro- and nano-patterned surfaces are brought into contact with fresh peritoneal samples. By comparing the forces measured, for a range of surface characteristics, data can be extracted which ultimately will lead to the design of an optimised custom manufactured surface patterning tailored specifically for use with peritoneal tissue.

## 3 Methods

### 3.1 Materials

#### 3.1.1 Peritoneum

The peritoneum provides the lining to the abdominal cavity, being composed of an outer layer of fibrous connective tissue upon which is a monolayer of mesothelial cells. It is the latter that comes into direct contact with and affects the adherence for the device. The mesothelium/peritoneum is one of the quickest healing organs in the human body, with re-peritonealisation of a traumatised surface being complete within 5 to 7 days post-trauma.

The surface is known to be hydrophilic in nature [20], and is covered with a thin layer of fluid which is secreted continuously from specialised cells within the peritoneum. This feature ensures that the peritoneal surface remains wet at all times. The major function of the fluid is to provide lubrication for the abdominal organs that it covers. However, for our purposes it is possible to exploit the presence of this fluid for capillary adhesion.

Traditional methods for analysing the peritoneum have largely been concerned with the types, contents and functions of the cells making up the tissue. Such light or electron microscopic analysis typically requires fixation and staining/labelling of the tissue. While allowing great insight into the cell biology and physiology of the peritoneum, these techniques disrupt the *in-vivo* architecture and as such do not present an accurate representation of the actual surface topography.

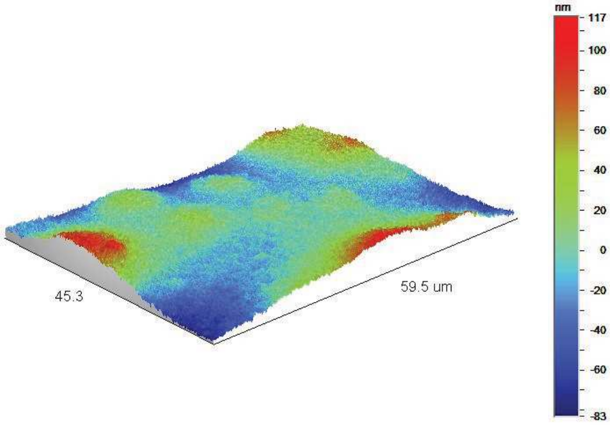


*Figure 3: Three dimensional white light interferometer image of mouse peritoneum, showing a height range of 200nm. The three raised areas are likely to represent the areas overlying individual cell nuclei.*

In order to overcome this white light interferometry was used to image sections of experimental mouse tissue (Fig. 3). The resulting images reveal a relatively flat surface, with a height range of the order of 200nm only, and defined raised areas at regular intervals. These areas correspond to the spacing of the nuclei towards the centre of each cell.

In all subsequent experiments rat peritoneum samples were used, these having been taken from the abdominal wall of rats dissected immediately post mortem within the University of Leeds' Biomedical Services. The animals were bred in-house for research purposes other than this study. The samples were placed immediately in phosphate buffer solution (PBS) at room temperature, in order to preserve structure and hydration. Experiments were carried out within 8 hours of tissue collection. The peritoneal surface of the abdominal wall sample could be easily identified as it had much more prominent blood vessels near the surface. It is generally recognised that rat peritoneum bears a close resemblance to a human tissue and it has been used as a proxy for this research.

### 3.1.2 Polymers

In order to investigate the physical properties required to enhance adhesion and friction of a surface at an interface with the peritoneum, a range of micro- and nano-patterned surfaces were analysed prior to being tested for adhesion and friction performance. Six manufactured polymer surfaces, Table 1, were acquired from MacDermid Autotype, and investigated along with a non-patterned "smooth" polymer. The patterns on the polymer surfaces P2-P6 have similar morphology; their topography consisting of regular S-waves in both the x and y planes, producing domes with a peak-to-peak spacing of 250 nm. The peaks, having different heights, and the associated polymer surfaces were manufactured from different materials and so have different hardness and elasticity properties. These patterns are contrasted with the pattern of polymer P1, which is comprised of four sided pyramids with a regular peak-to-peak spacing of 4 μm and a much greater height (approx 2.8 μm). Polymer P7 is a smooth unpatterned surface. A scanning electron microscopy was initially used to gain a basic understanding of the scale and dimensions of the surfaces. They were then observed in closer detail using atomic force microscopy, which enabled the height dimensions and roughness of the surface details to be assessed. Measures of material hardness and elasticity were taken with a nano-indentation instrument (MicroMaterials Ltd).

*Table 1: AFM surface morphology measurements.*

| Polymer | Scan area ($\mu m^2$) | Height range (nm) | Average height (nm) | Roughness Ra (nm) |
|---|---|---|---|---|
| P1 | 400 | 2826.6 | 1127.0 | 530.2 |
| P2 | 400 | 66.9 | 31.8 | 12.3 |
| | 25 | 129.8 | 73.0 | 21.4 |
| P3 | 400 | 141.8 | 80.4 | 18.8 |
| | 100 | 91.4 | 45.9 | 15.4 |
| | 25 | 101.8 | 50.2 | 19.4 |
| P4 | 400 | 78.9 | 39.4 | 12.2 |
| | 100 | 92.9 | 62.0 | 15.8 |
| | 25 | 95.0 | 54.5 | 17.5 |
| P5 | 400 | 135.5 | 64.9 | 18.2 |
| | 100 | 84.1 | 41.4 | 13.4 |
| | 25 | 86.2 | 40.5 | 14.0 |
| P6 | 400 | 138.7 | 86.8 | 18.7 |
| | 100 | 110.61 | 53.28 | 15.74 |
| | 25 | 118.4 | 56.82 | 16.54 |
| P7 | 100 | 33.76 | 16.93 | 3.27 |

The nano-indentation measurements showed some clear differences in the material properties analysed, with polymer surfaces P6 and P7 having the highest hardness and polymers P1 and P4 being at the other end of the scale, see Table 2.

*Table 2: Mechanical properties of polymers obtained from nano-indentation experiments.*

| Polymer | Hardness (GPa) | Reduced modulus (GPa) |
|---|---|---|
| P1 | 0.031 | 0.458 |
| P2 | 0.177 | 2.162 |
| P3 | 0.209 | 2.749 |
| P4 | 0.076 | 0.939 |
| P5 | 0.154 | 1.770 |
| P6 | 0.376 | 3.759 |
| P7 | 0.428 | 4.888 |

### 3.2 Experimental setup

Adhesion tests were carried out using a MUST (Modular Universal Surface Tester) rig manufactured by Falex Tribology company [21]. For measurements of forces in the mili-Newton range a force transducer was used, which consists of a cantilever based on a parallel spring system (Fig. 4).

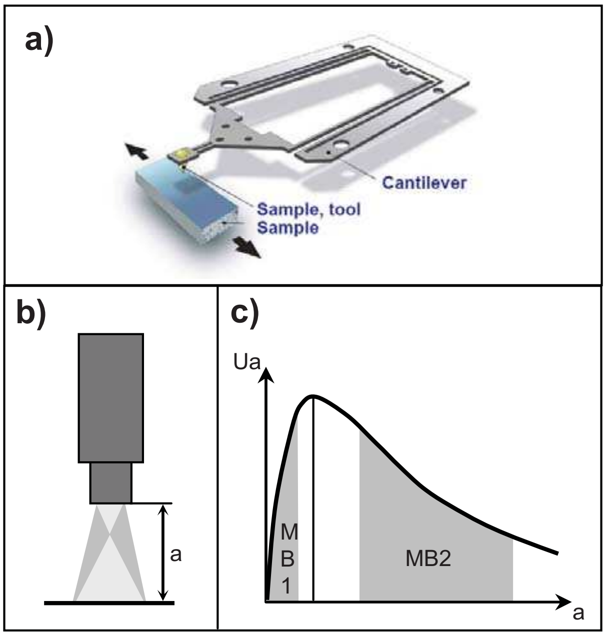


*Figure 4: Functional principle of the force transducer; a) cantilever; b) fibre optic sensor; c) fibre optic sensor measurement characteristic – explained in the text.*

In this study, a modified version of a cantilever was employed, which was able to deflect in the indentation direction only. The cantilever was fixed in a mechanical carrier. For deflection measurement of the cantilever, a fibre optic sensor (FOS) was used. A micro-mirror was fixed to the moving part of the cantilever which acted as a reflective surface for the FOS. At the tip of the FOS, two glass fibre bundles were joined. The light radiated from the first one – the transmission light conductor bundle – was reflected on a mirror and captured by the second receiving light conductor bundle. The captured light was then converted by opto-electronic transducers to an electrical signal and sent to the data acquisition unit. The sensing rate characteristic, Ua = f(a), was determined by the photometric distance law (Fig. 4c) and, depending on the measurement resolution required, the sensor could be operated over one of two measuring ranges: MB1 and MB2.

Samples of rat peritoneum were mounted in opposition to the test polymers, which in turn were mounted on the cantilever part of the instrument. The samples were arranged so that the interface of the two surfaces was perpendicular to the movement of the instrument, thereby allowing direct indentation tests. 4mm discs (12.57mm$^2$) of the test polymers were used throughout, apart from the specific surface area tests.

### 4 Results

Each indentation cycle using the MUST instrument generated a Force-Distance curve for the forces acting at the polymer-peritoneum interface. A representative curve is given in Fig. 5.

The test was started at point A, as the surfaces are brought together. At point B they have come within a distance small enough to allow an interfacial attractive force to produce a ‘snap-in’ effect and the polymer is pulled onto the peritoneum. Contact is made at point C as a result of the ‘snap-in’. The polymer then continues to be pushed into the soft peritoneum at a uniform rate until the pre-defined loading force is reached at point D. The slope CD is dependent of the spring constant within the cantilever and the elastic modulus of the peritoneal surface. At point D the instrument’s motion is reversed so that it acts to separate the surfaces. However, it can be seen that the polymer stays in contact even as the tangential force acting upon it becomes negative. This indicates an adhesive force at the interface, whose maximum value is at E. The slope DE differs from CD, demonstrating the visco-elastic nature of the peritoneum. As the adhesive force is overcome and the polymer is released the separating force returns to zero. F marks the point at which separation of the surfaces is complete. The slope EF is rarely vertical, indicating a gradual separation.

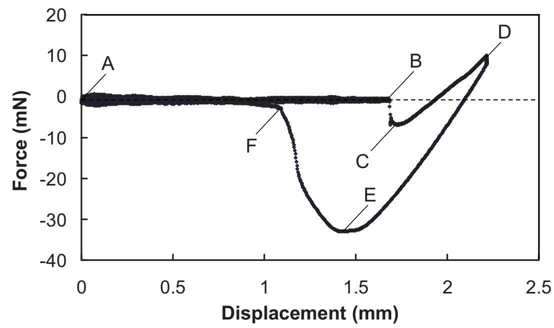


*Figure 5: Example of a typical displacement-force curve; A-F explained in the text.*

Each polymer went through five indentation cycles with a peritoneal sample and good experimental repeatability achieved. The curves for polymers P3 and P6 are shown below in Fig. 6 and 7.

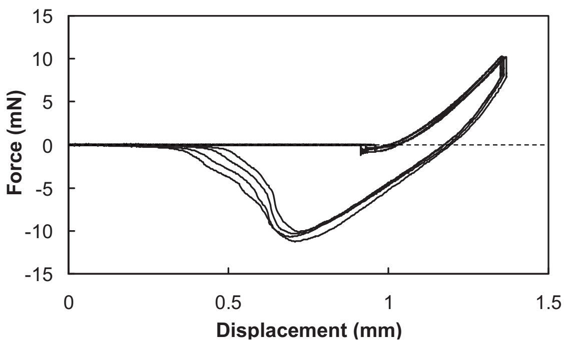


*Figure 6: Series of single indents repeated for polymer P3 sample.*

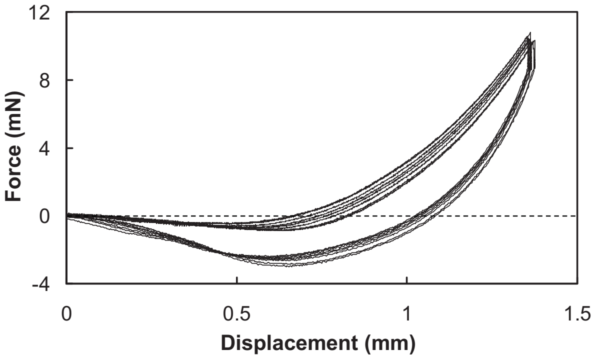


*Figure 7: Series of single indents repeated for polymer P6 sample.*

Different shapes of displacement-force curves were observed for each polymer type. This is further demonstrated in Fig. 8.

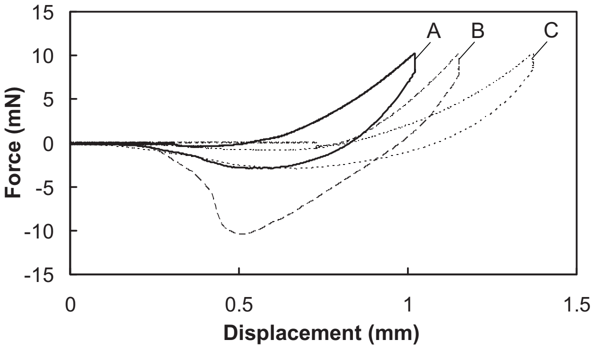


*Figure 8: Representative three different types of displacement-force curves recorded for A: polymer P5, B: polymer P3, C: polymer P6.*

The maximum adhesion force was found for each polymer. Three indentations at different locations on the peritoneal sample were performed. This was done with the interface at 90 degrees to the movement of the instrument, and again with the interface at 45 degrees. The results are shown in Fig. 9 and 10.

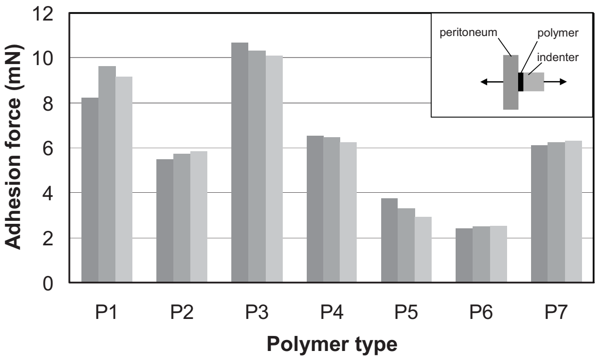


*Figure 9: 90deg adhesion force measurements for tested polymer samples.*

The results at 90 degree adhesion are more uniform than those obtained for the 45 degree tests. Greatest adhesion, at 90 degrees, was achieved by polymers P1 and P3; interestingly the same polymers achieved the lowest adhesion forces at 45 degrees.

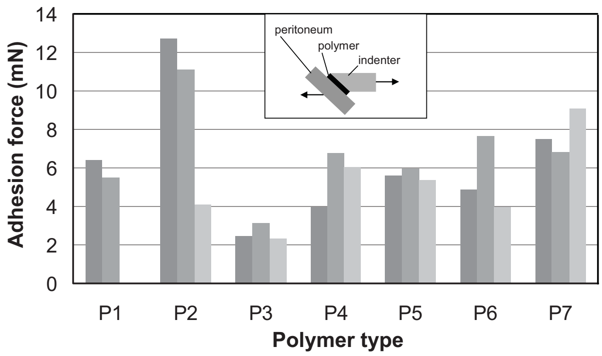


*Figure 10: 45deg adhesion force measurements for tested polymer samples.*

In the design of the eventual device, a requirement is that the adhesion mechanism for a given surface area will hold a predicted mass. It is therefore essential that the adhesive properties scale up in direct proportion to the contact area. A range of surface areas of polymer P3 was explored as an exemplar. Fig. 11 demonstrates that, over the range investigated, the adhesion force generated is indeed directly proportional to the contact area.

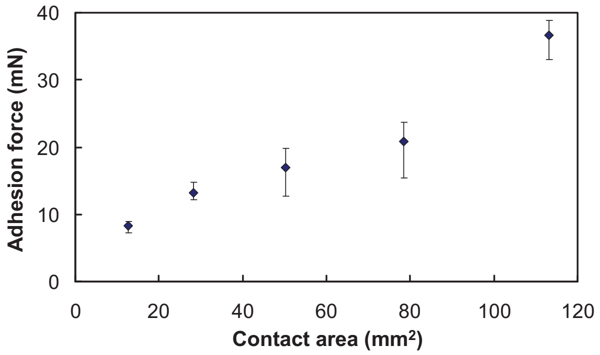


*Figure 11: Adhesion force as a function of indenter contact area measured for polymer P3.*

## 5 Discussion

The study shows the potential of nano-patterned surfaces to generate the adhesion necessary for a miniature device to maintain contact with a wet peritoneal surface. Using areas of 12.57mm$^2$ adhesion forces of up to 10mN have been achieved. This can be expressed as 795.5 N/m$^2$. If this adhesive force can be scaled up in proportion, an area of 400mm$^2$ would be able to hold a device of approximately 32g. This is an encouraging finding given that these polymers were not specifically designed for providing maximum adhesion.

Although as yet it has not been possible to show a particular link between a specific surface pattern and adhesion, it is seen that each of the polymer surfaces investigated results in a different shaped displacement-force curve. It is especially interesting to observe a different shaped curve for different polymers during the unloading cycle, revealing a different dynamic response (Fig. 8). By determining the area of the curve for negative force values, the adhesion work can be worked out and compared for each polymer, which will help in future studies when designing the motion mechanism for the intra-abdominal device.

From Fig. 9 and 10, it can be observed that there is a negative correlation between results observed for 90deg and 45deg adhesion force measurements. Polymers, which demonstrated the best performance in the 90deg tests, showed very poor adhesive properties during the 45deg tests. This is an interesting behaviour, which has to be related to the geometrical properties of polymeric contact surfaces investigated.

It is demonstrated that the adhesive force generated does indeed appear to increase in a way directly proportional to the contacting surface area. However, it has only been possible to show this is true up to 120mm$^2$. At larger surface areas this relationship may well be violated as possible contact points become saturated. This will be investigated in future work as will the case of what forces are required to maintain contact when there is relative motion between the contacting surface and the peritoneum.

## 6 Conclusions

The adhesive forces needed to enable a small mobile device to remain in contact with the abdominal cavity wall have been explored from the point of view of using biomimetic principles in the form of structured polymer surfaces to provide the necessary level of adhesion required. From the results obtained the following conclusions can be drawn:

- The peritoneum forming the abdominal wall tissue, is characterised by a relatively flat surface with a height range of the order of 200nm; it is hydrophilic in nature, remaining wet at all times, which allows the presence of the fluid for the purpose of capillary adhesion to be exploited.
- It is shown that the geometrical pattern on the polymer samples has a significant impact on the adhesion force generated which depends on the patternation present; the minimum recorded force was equal to 2mN and the maximum equal to12mN.
- If for the maximum adhesive force achieved, 12mN, the associated contact area were scaled up to 400mm$^2$, it would be able to support a device of approximately 32g, which is a representative of the mass of a small intra-abdominal device.
- It is found that the adhesive properties of the representative polymers investigated scale in direct proportion to the contact area.
- A negative correlation between results for 90deg and 45deg adhesion force measurements is observed; polymers with the highest adhesion at 90deg show the lowest adhesion at 45deg.
- It has been observed that each polymer leads to a different shaped displacement-force curve revealing a different dynamic response of the system and allowing for future analysis of the motion mechanism for the intra-abdominal device.
- The experimental method used has proved capable of providing repeatable adhesion force measurements, showing not only quantitative but also qualitative differences between the material surfaces tested.

## 7 Acknowledgements

The authors wish to thank MacDermid Autotype for making and providing the nanostructured polymer samples used in the study and the Falex Tribology company for providing a modified cantilever system for the adhesion experiments.

## 8 References

[1] Perissat, J., Collet, D., Belliard, R., Desplantez, J., & Magne, E. 1992, "Laparoscopic cholecystectomy: the state of the art. A report on 700 consecutive cases", World J.Surg., vol. 16, no. 6, pp. 1074-1082.

[2] Guillou, P. J., Quirke, P., Thorpe, H., Walker, J., Jayne, D. G., Smith, A. M., Heath, R. M., & Brown, J. M. 2005, "Short-term endpoints of conventional versus laparoscopic-assisted surgery in patients with colorectal cancer (MRC CLASICC trial): multicentre, randomised controlled trial", Lancet, vol. 365, no. 9472, pp. 1718-1726.

[3] Ballantyne, G. H. 2002, "Robotic surgery, telerobotic surgery, telepresence, and telementoring. Review of early clinical results", Surg. Endosc., vol. 16, no. 10, pp. 1389-1402.

[4] Pott, P. P., Scharf, H. P., & Schwarz, M. L. 2005, "Today's state of the art in surgical robotics*", Comput.Aided Surg., vol. 10, no. 2, pp. 101-132.

[5] Kobayashi Y., Chiyoda S., Watabe K., Masafumi O., & Nakamura Y. 2007, "Small occupancy robotic mechanisms for endoscopic surgery.", 5th International Conference on Medical Image Computing and Computer Assisted Intervention.LNCS, vol. 2488, pp. 75-82.

[6] Ikuta K., D. S. H. T. H. H. 2007, "Hyper-finger for remote minimally invasive surgery in deep area.", Medical Image Computing and Computer-Assisted Intervention - MICCAI 2002: 5th International Conference, Tokyo, Japan.

[7] T. Ota, N. A. Patronik, C. N. Riviere, and M. A. Zenati, "Minimally invasive epicardial injections using a novel semi-autonomous robotic device," Circulation, 2008. 118:S115–S120.

[8] Rentschler, M. E., Dumpert, J., Platt, S. R., Ahmed, S. I., Farritor, S. M., & Oleynikov, D. 2006, "Mobile in vivo camera robots provide sole visual feedback for abdominal exploration and cholecystectomy", Surg.Endosc., vol. 20, no. 1, pp. 135-138.

[9] Menciassi, A., Stefanini, C., Orlandi, G., Quirini, M., & Dario, P. 2006, "Towards active capsular endoscopy: preliminary results on a legged platform", Conf.Proc.IEEE Eng Med.Biol.Soc., vol. 1, pp. 2215-2218.

[10] Kassim, I., Phee, L., Ng, W. S., Gong, F., Dario, P., & Mosse, C. A. 2006, "Locomotion techniques for robotic colonoscopy", IEEE Eng Med.Biol.Mag., vol. 25, no. 3, pp. 49-56.

[11] www.theodora.com/anatomy

[12] Cheung E, Karagozler ME, Park S, Kim B, Sitti M. A new endoscopic microcapsule robot using beetle inspired microfibrillar adhesives. 2005 IEEE/ASME Int. Conf. Advanced Intelligent Mechatronics: 551-557.

[13] 2. Federle W, Barnes WJP, Baumgartner W, Drechsler P, Smith JM. Wet but not slippery: boundary friction in tree frog adhesive toe pads. J. R. Soc. Interface. 2006; 3 (10): 689-687.

[14] 3. Autumn K, Sitti M, Liang YA, Peattie AM, Hansen WR, Sponberg S, Kenny TW, Fearing R, Israelachvili JN, Full RJ. Evidence for van der Waals adhesion in Gecko setae. PNAS 2002; 99 (19): 12252-12256.

[15] SJ Abbott, PH Gaskell. Mass production of bio-inspired structured surfaces. Proc. IMechE Vol. 221 Part C: J. Mechanical Engineering Science. 2007: 1181-1191.

[16] AK Geim, SZ Dubonos, IV Grigorieva, KS Novoselov, AA Zhukov, S Yu Shapoval. Microfabricated adhesive mimicking gecko foot hair. Nature Materials 2003; Vol. 2: 461-463.

[17] SN Gorb, M Sinha, A Peressadko, KA Daltorio, RD Quinn. Insects did it first: a micropatterned adhesive tape for robotic applications. Bioinspiration & Biomimetics. 2007; Vol. 2: S117–S125.

[18] J Kwon, E Cheung, S Park, M Sitti. Friction enhancement via micro-patterned wet elastomer adhesives on small intestinal surfaces. Biomedical Materials. 2006; Vol 1: 216–220.

[19] A Mahdavi, L Ferreira, C Sundback, JW Nichol, EP Chan, DJD Carter, CJ Bettinger, S Patanavanich, L Chignozha, E Ben-Joseph, A Galakatos, H Pryor, I Pomerantseva, PT Masiakos, W Faquin, A Zumbuehl, S Hong, J Borenstein, J Vacanti, R Langer, JM Karp. A biodegradable and biocompatible gecko-inspired tissue adhesive. PNAS. 2008 ; vol. 105 (7): 2307–2312.

[20] C. Gómez-Suárez, G. M. Bruinsma, G. Rakhorst, H. C. van der Mei and H. J. Busscher; Hydrophobicity of Peritoneal Tissues in the Rat. Journal of Colloid and Interface Science 253, 470–471 (2002).

[21] S. Achanta, D. Drees and J.-P. Celis, “Friction and nanowear of hard coatings in reciprocating sliding at milli-Newton loads”, Wear, 259 (2005), pp. 719-729.